J. Fluid Mech. (1994), *vol.* 262, *pp.* 265–291

On the subharmonic instabilities of steady three-dimensional deep water waves

By MANSOUR IOUALALEN† AND CHRISTIAN KHARIF

Institut de Mécanique Statistique de la Turbulence, 12 avenue de Général Leclerc, 13003 Marseilles, France

(Received 22 March 1993)

A numerical procedure has been developed to study the linear stability of nonlinear three-dimensional progressive gravity waves on deep water. The three-dimensional patterns considered herein are short-crested waves which may be produced by two progressive plane waves propagating at an oblique angle, γ, to each other. It is shown that for moderate wave steepness the dominant resonances are sideband-type instabilities in the direction of propagation and, depending on the value of γ, also in the transverse direction. It is also shown that three-dimensional progressive gravity waves are less unstable than two-dimensional progressive gravity waves.

1. Introduction

The present study extends the work of many authors on the stability of two-dimensional progressive and standing waves to three-dimensional waves of finite amplitude. While the former waves have been intensively analysed, up to now the latter have been the object of very few studies. The stability of two-dimensional progressive Stokes waves which are periodic, irrotational surface waves propagating under the influence of gravity has been investigated by Benjamin & Feir (1967). Using a perturbation method, they showed that a weakly nonlinear wave train is unstable to modulational perturbations. In other words, a Stokes wave of wave steepness ak and frequency ω is unstable to two-dimensional perturbations of frequency $\omega(1 \pm \delta)$ when $0 \leqslant \delta \leqslant \sqrt{2}ak$. The maximum growth rate is obtained for $\delta = ak$. This instability produces an amplitude modulation of the original wave train. The instability of a two-dimensional uniform wave train to three-dimensional perturbations was shown by Zakharov (1968), using the nonlinear Schrödinger equation.

Longuet-Higgins (1978*a*, *b*) extended numerically the investigation of the stability of finite-amplitude Stoke waves up to $ak = 0.42$ to superharmonic and subharmonic disturbances. He showed that Stokes waves are marginally stable to superharmonic perturbations and discovered that when the wave steepness reached the value of $ak = 0.405$ subharmonic disturbances of twice the wavelength of the unperturbed wave and travelling with the same speed become unstable. McLean *et al.* (1981) and McLean (1982) considered the stability of finite-amplitude Stokes waves up to $ak = 0.41$ to three-dimensional perturbations using a collocation method; they established that for amplitudes smaller than $h = 0.30$, the dominant instability is two-dimensional while for larger amplitudes it becomes three-dimensional. Extending McLean's work, Kharif (1987) showed that the instabilities are no longer predominantly three-dimensional when the wave steepness reaches a value of approximately $ak = 0.429$. Recently Kharif & Ramamonjiarisoa (1988, 1990) reported an important result concerning the relative

† Present address: ORSTOM BP A5, Nouméa Cedex, New Caledonia, France.

strength of McLean's class I and class II instabilities for basic wave steepness larger than 0.41 and predicted new two-dimensional superharmonic instabilities utilizing the condition of instability of MacKay & Saffman (1986). Their work completed the study of the linear stability of Stokes waves.

In the case of two-dimensional standing waves little has been done except for the work of Okamura (1984, 1986) who considered the instability of weakly nonlinear standing waves using Zakharov's equation and Mercer & Roberts (1992) who very recently considered finite-amplitude standing waves on deep water. In the latter it was shown that all but very steep standing waves are generally stable to harmonic perturbations and unstable to subharmonic perturbations. From these studies we now have useful results concerning two limits of three-dimensional gravity waves, that is, two-dimensional progressive waves and two-dimensional standing waves.

While the stability of two-dimensional water waves to infinitesimal disturbances has been intensively analysed, the stability of three-dimensional waves has for the most part been ignored. The work of Ioualalen & Kharif (1993) is an exception. The present investigation extends the latter stability analysis of approximate three-dimensional doubly periodic surface gravity waves of permanent form on water of infinite depth to subharmonic disturbances.

The three-dimensional waves considered herein are short-crested waves which may be produced by two progressive plane waves propagating at an oblique angle to each other or by a sea-wall reflection of a plane progressive wave. Many authors have calculated analytically or numerically these forms. In a linear description, the short-crested waves are obtained by a superposition of the linear progressive surface wave solutions. Fuchs (1952) was the first to obtain second-order solutions while Chappelear (1961) extended them to third order. Using a different perturbation parameter Hsu, Tsuchiya & Silvester (1979) calculated a third-order expansion in a dimensionless form. With the aid of an algebraic manipulator Ioualalen (1993) extended the formal power expansions to fourth and fifth orders. Roberts (1983) computed numerically high-order solutions using also a perturbation method. Fully numerical methods have been developed by Roberts & Schwartz (1983) and Bryant (1985) to calculate highly nonlinear short-crested waves. In the limit in which the length of the wave crests become long, Roberts & Peregrine (1983) obtained an analytic solution to fourth order. In elucidating some of the highly nonlinear properties of steadily propagating short-crested waves Roberts (1983) discovered the occurrence of a doubly infinite family of harmonic resonances which cause the perturbation series to have a zero radius of convergence everywhere. However, he showed that useful results can still be extracted from a perturbation series which involves harmonic resonances. Although the resonances are densely distributed, almost all of them are of very high order. These very-high order resonances contribute to the fine structure of the solutions and the error produced by truncating the expansion at an order N and thus ignoring such details is at most $(ak)^{N/3}$ where ak is the wave steepness. Roberts (1983) showed that the singularities due to the harmonic resonances are extremely weak and do not in any way affect the coefficients of a finite truncation of the perturbation series. Numerical calculations by Roberts (1983) have revealed the occurrence of pole-zero pairs extremely close to one another, establishing the weakness of the resonant structures.

Ioualalen & Kharif (1993) computed the stability of these fully three-dimensional surface gravity waves to superharmonic disturbances in order to evaluate the timescales of these resonances and discovered that the associated instabilities are sporadic bubbles of instability due to the collision of superharmonic modes and correspond to weak three-dimensional extensions of McLean's class I instabilities. The

main purpose of this paper is to study the linear stability of short-crested waves to evaluate their initial behaviour and also to compare subharmonic instabilities to superharmonic instabilities. Following Roberts (1983) and Ioualalen (1990) the basic waves are numerically calculated using a high-order perturbation expansion. Convergence acceleration techniques, like the ρ-method developed by Gilewicz (1978) selecting the best Padé approximant, are applied to amplitude expansions in order to obtain solutions for amplitudes up to and past the singularities. As in Ioualalen & Kharif (1993), the eigenvalue problem derived from the stability analysis of three-dimensional waves is numerically solved using collocation and Galerkin methods. Both methods are compared and it is shown that the Galerkin one is more efficient to treat three-dimensional wave patterns. A classification of the instabilities is carried out, superharmonic and subharmonic instabilities are compared and maximum growth rates and frequencies are computed.

2. Mathematical formulation

We consider surface gravity waves on an inviscid incompressible fluid of infinite depth. The flow is assumed irrotational. The governing equations are

$$\nabla^2\phi = 0, \quad z \leqslant \eta(x, y, t), \tag{2.1}$$

$$\lim_{z\to-\infty} \phi = 0, \tag{2.2}$$

$$\left.\begin{aligned} \phi_t + \eta + \tfrac{1}{2}(\phi_x^2 + \phi_y^2 + \phi_z^2) &= 0, \\ \eta_t + \phi_x\eta_x + \phi_y\eta_y - \phi_z &= 0, \end{aligned}\right\} \quad z = \eta(x, y, t), \tag{2.3, 2.4}$$

where $\phi(x, y, z, t)$ is the velocity potential and $z = \eta(x, y, t)$ the equation of the free surface. The classical equations (2.1)–(2.4) are given in a dimensionless form which is equivalent to setting $g = k = 1$, where g is the gravitational acceleration and k the wavenumber of both incident wave trains. Now let h denote the wave steepness instead of ak.

Following Roberts (1983) we define

$$X = x\sin\theta - \omega t, \quad Y = y\cos\theta, \quad Z = z,$$

where ω is the frequency and θ the angle between the direction of propagation of the incident wave and the normal to the sea wall: $\theta = \frac{1}{2}(\pi - \gamma)$. The values $\theta = 90°$ and $\theta = 0°$ correspond respectively to Stokes' progressive waves and fully reflected standing waves. Both are two-dimensional limiting forms of short-crested waves. The angle θ characterizes the three-dimensionality level of the flow.

The solutions of Laplace's equation (2.1) must satisfy the condition (2.2) and the nonlinear conditions (2.3) and (2.4) on the free surface. Progressive waves in deep water which are periodic in two orthogonal directions and are steady relative to a frame of reference moving in one of these directions are given by Roberts (1983) and Ioualalen (1990) as doubly periodic Fourier series using a perturbation expansion in the wave steepness, h, up to 27th order. The velocity potential and free-surface elevation of unperturbed waves are respectively denoted by $\bar{\phi}(X, Y, Z)$ and $\bar{\eta}(X, Y)$. The wave steepness of the basic wave is defined by

$$h = \tfrac{1}{2}\{\bar{\eta}(0, 0) - \bar{\eta}(\pi, 0)\},$$

which is half of the non-dimensional peak-to-trough height since the peak of the wave will be fixed at $(X, Y) = (0, 0)$.

We seek expressions for the velocity potential, the surface elevation and the frequency of the form

$$\bar{\phi} = \sum_{i=1}^{\infty} \sum_{m,n} d_{i,mn} \sin(mX) \cos(nY) \exp(\gamma_{mn} Z) h^i,$$

$$\bar{\eta} = \sum_{i=1}^{\infty} \sum_{m,n} c_{i,mn} \cos(mX) \cos(nY) h^i,$$

$$\omega = \sum_{i=0}^{\infty} \omega_i h^i,$$

$$\alpha = \sin\theta, \quad \beta = \cos\theta, \quad \gamma_{mn} = (m^2\alpha^2 + n^2\beta^2)^{\frac{1}{2}}.$$

The symmetry and the nonlinearity in the wave require that the indices i, m and n be of the same parity.

Figure 1 displays short-crested water waves for $\theta = 80°$ and $45°$. For $\theta = 80°$ the waves are long-crested due to the proximity of $\theta = 90°$ and for $\theta = 45°$ the waves are fully three-dimensional.

Now consider a frame of reference (x^*, y^*, z^*) where

$$x^* = x - ct, \quad c = \omega/\alpha, \quad y^* = y, \quad z^* = z.$$

In this reference frame moving in the x-direction with the speed c, the short-crested waves are steady. The velocity potential, ϕ^*, in this frame is related to ϕ by

$$\phi^* = \phi - cx.$$

For simplicity asterisks are omitted hereafter.

The main purpose of the present investigation is to study the stability of approximate three-dimensional waves, propagating in the x-direction without change of shape, to infinitesimal disturbances. Let

$$\eta(x, y, t) = \bar{\eta}(x, y) + \eta'(x, y, t), \tag{2.5}$$

$$\phi(x, y, z, t) = \bar{\phi}(x, y, z) + \phi'(x, y, z, t), \tag{2.6}$$

where $(\bar{\eta}, \bar{\phi})$ and (η', ϕ') correspond, respectively, to the unperturbed and infinitesimal perturbative motions $(\eta' \ll \bar{\eta}, \phi' \ll \bar{\phi})$.

After substituting (2.5) and (2.6) into (2.3) and (2.4), recasting them in the new coordinate system and linearizing, we obtain the first-order perturbation equations

$$\nabla^2 \phi' = 0, \quad z \leqslant \bar{\eta}(x, y), \tag{2.7}$$

$$\lim_{z \to -\infty} \phi' = 0, \tag{2.8}$$

$$\left.\begin{aligned} \phi'_t &= -\bar{\phi}_x \phi'_x - \bar{\phi}_y \phi'_y - \bar{\phi}_z \phi'_z - (1 + \bar{\phi}_x \bar{\phi}_{xz} + \bar{\phi}_y \bar{\phi}_{yz} + \bar{\phi}_z \bar{\phi}_{zz}) \eta', \\ \eta'_t &= (\bar{\phi}_{zz} - \bar{\eta}_x \bar{\phi}_{xz} - \bar{\eta}_y \bar{\phi}_{yz}) \eta' - \bar{\eta}_x \phi'_x - \bar{\phi}_x \eta'_x - \bar{\eta}_y \phi'_y - \bar{\phi}_y \eta'_y + \phi'_z, \end{aligned}\right\} \quad z = \bar{\eta}(x, y). \tag{2.9, 2.10}$$

Extending the procedure of Ioualalen & Kharif (1993) to subharmonic disturbances, we look for non-trivial solutions of (2.9) and (2.10) of the form

$$\begin{pmatrix} \eta' \\ \phi' \end{pmatrix} = \mathrm{e}^{-\mathrm{i}\sigma t} \mathrm{e}^{\mathrm{i}(px+qy)} \begin{pmatrix} \sum_{J=-\infty}^{\infty} \sum_{K=-\infty}^{\infty} a_{JK} \mathrm{e}^{\mathrm{i}(J\alpha x + K\beta y)} \\ \sum_{J=-\infty}^{\infty} \sum_{K=-\infty}^{\infty} b_{JK} \mathrm{e}^{\mathrm{i}(J\alpha x + K\beta y)} \mathrm{e}^{\kappa_{JK} z} \end{pmatrix}, \tag{2.11}$$

where $\kappa_{JK} = [(p + J\alpha)^2 + (q + K\beta)^2]^{\frac{1}{2}}$.

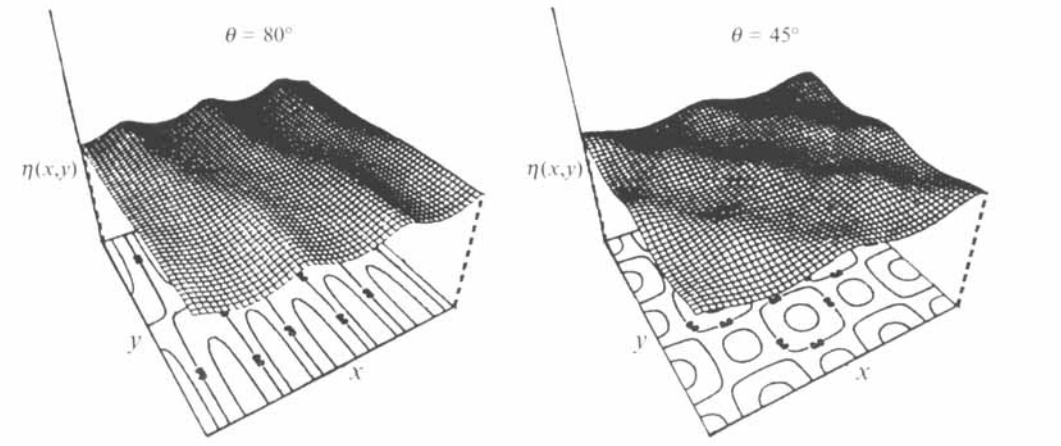

FIGURE 1. Free surface of short-crested water waves for $h = 0.30$.

If $p = N\alpha$ and $q = M\beta$ with $(N, M) \in N^2$, then the wavelengths in the x-direction and y-direction of the perturbation are the same, respectively, as the longitudinal wavelength and the transversal wavelength of the basic wave and the perturbation is called superharmonic. If $p \neq N\alpha$ and $q \neq N\beta$, then in general the perturbation contains components with wavelengths in the x-direction and y-direction which are greater than, respectively, the longitudinal wavelength and the transversal wavelength of the basic wave and the perturbation is called subharmonic. There are also perturbations subharmonic in one direction and superharmonic in the other.

The coefficients a_{JK}, b_{JK} and the eigenvalue σ, the frequency of the perturbations relative to the three-dimensional basic wave, are to be determined. Since the system of equations (2.7)–(2.10) is real valued the eigenvalues σ appear in complex-conjugate pairs. Thus instability corresponds to $\mathrm{Im}(\sigma) \neq 0$.

For $h = 0$, the unperturbed wave is given by $\bar{\eta} = 0$ and $\bar{\phi} = -c_0 x$ with $c_0 = 1/\alpha$ being the celerity of the wave. Then the eigenvalues are

$$\sigma^s_{JK} = -(p + J\alpha)\, c_0 + s[(p + J\alpha)^2 + (q + K\beta)^2]^{\frac{1}{4}}, \quad s = \pm 1.$$

The sign of s determines the direction of propagation of the disturbance relative to a frame of reference moving with the speed c_0. Note also that there exists a degeneracy with respect to p and q since

$$\sigma^s_{JK}(p, q) = \sigma^s_{J-M,\, K-N}(p + \alpha M, q + \beta N), \quad (M, N) \in N^2.$$

As noted by McLean (1982) this degeneracy is artificial since the corresponding eigenvectors are physically the same. This degeneracy is removed by restricting p and q to the ranges $0 \leqslant p < \alpha$ and $0 \leqslant q < \beta$.

The set of eigenvalues $\{\sigma^s_{JK}\}$ is spectrally stable for $h = 0$. Instabilities can arise when the parameter h increases. Recently, MacKay & Saffman (1986), taking advantage of fundamental work on Hamiltonian systems, formulated a necessary condition for instability in terms of the coalescence of two eigenvalues of opposite signatures or at zero frequency. A change from stability to instability can occur only if, for some h, two modes have the same frequency:

$$\sigma^s_{J_1 K_1}(p, q, h) = \sigma^{s'}_{J_2 K_2}(p, q, h).$$

In a linear approximation this loss of stability may be written in the following form:

$$\left[\alpha^2\left(\frac{p}{\alpha} + J_1\right)^2 + \beta^2\left(\frac{q}{\beta} + K_1\right)^2\right]^{\frac{1}{4}} + \left[\alpha^2\left(\frac{p}{\alpha} + J_2\right)^2 + \beta^2\left(\frac{q}{\beta} + K_2\right)^2\right]^{\frac{1}{4}} = J_1 - J_2, \qquad (2.12)$$

with $s_1 = -s_2 - 1$.

The coalescence of two eigenvalues may be interpreted as a resonance between two infinitesimal modes of wave vectors $\boldsymbol{k}_1$ and $\boldsymbol{k}_2$ and the basic wave with fundamental eigenvectors $\boldsymbol{k}_{01}$ and $\boldsymbol{k}_{02}$. These conditions given by Phillips (1960) are

$$\boldsymbol{k}_1 \pm \boldsymbol{k}_2 = \sum_i \pm \boldsymbol{k}_{0i}, \qquad \omega_1' \pm \omega_2' = \sum_i \pm \omega_{0i}',$$

with $i = 1, 2$, at least for gravity waves, where ω_1', ω_2' and ω_{0i}' represent, respectively, the frequencies of the disturbances and the frequencies of the unperturbed wave in a fixed frame of reference.

The choice of $\boldsymbol{k}_1$ and $\boldsymbol{k}_2$ leads to the different classes of instabilities. Following McLean (1982) we define two general classes from (2.12): class I corresponds to $(J_1 - J_2)$ even and class II corresponds to $(J_1 - J_2)$ odd. The degeneracy noted previously allows us to choose J_1 and J_2 such that

and
$$\left.\begin{array}{l} J_1 = j, J_2 = -j \text{ for the class I}(j) \\ J_1 = j, J_2 = -j-1 \text{ for the class II}(j) \end{array}\right\}, \quad j = 1, 2, 3, \ldots.$$

The present study will be limited to class I and class II for $j = 1$ which corresponds to the dominant resonances. Over the range considered herein, $0 \leqslant h \leqslant 0.30$, the higher-order resonances ($j = 2, 3, \ldots$) are very weak as suggested by Zakharov (1968). Then the symmetry and the nonlinearity in the basic wave require K_1 and K_2 to satisfy

and
$$\begin{array}{l} K_1 = \pm 1 \text{ and } K_2 = \pm 1 \text{ for class I} \\ K_1 = \pm 1 \text{ and } K_2 = \pm 2 \text{ for class II.} \end{array}$$

Class Ia ($j = 1, K_1 = K_2 = 1$) *or class Ia'* ($j = 1, K_1 = K_2 = -1$)

For class Ia equation (2.12) may be written in the following form

$$[(p+\alpha)^2 + (q+\beta)^2]^{\frac{1}{4}} + [(p-\alpha)^2 + (q+\beta)^2]^{\frac{1}{4}} = 2. \tag{2.13}$$

If we let $P = p$ and $Q = q + \beta$, then (2.13) becomes

$$[(P+\alpha)^2 + Q^2]^{\frac{1}{4}} + [(P-\alpha)^2 + Q^2]^{\frac{1}{4}} = 2.$$

In the (P, Q)-plane the resonance curves for class Ia are symmetrical about the P-axis and the Q-axis. So symmetry allow us to limit the study to $P \geqslant 0$ and $Q \geqslant 0$. The geometrical interpretation derived from resonance conditions is plotted in figure 2(a) with

$$\boldsymbol{k}_1 = \boldsymbol{k}_2 + \boldsymbol{k}_{01} + \boldsymbol{k}_{02}$$

and
$$\omega_1' = \omega_2' + 2\omega_0',$$

with $\boldsymbol{k}_1 = (p+\alpha, q+\beta)^t$, $\boldsymbol{k}_2 = (p-\alpha, q+\beta)^t$; $\boldsymbol{k}_{01} = \boldsymbol{k}_0^+ = (\alpha, \beta)^t$, $\boldsymbol{k}_{02} = \boldsymbol{k}_0^- = (\alpha, -\beta)^t$.

The frequencies in a fixed frame of reference are

$$\begin{aligned} \omega_1' &= |\boldsymbol{k}_1|^{\frac{1}{2}} = [(p+\alpha)^2 + (q+\beta)^2]^{\frac{1}{4}}, \\ \omega_2' &= -|\boldsymbol{k}_2|^{\frac{1}{2}} = -[(p-\alpha)^2 + (q+\beta)^2]^{\frac{1}{4}}, \\ \omega_0' &= |\boldsymbol{k}_{01}|^{\frac{1}{2}} = |\boldsymbol{k}_{02}|^{\frac{1}{2}} = 1. \end{aligned}$$

Figure 2(b) displays the resonance curves for different angles θ plotted from the relation (2.13). Class Ia' and class Ia are symmetrical about the p-axis. Note that $\theta = 90°$ corresponds to class I ($N = 2$) in figure 1 of McLean (1982).

Class Ib ($j = 1, K_1 = 1, K_2 = -1$) *or class Ib'* ($j = 1, K_1 = -1, K_2 = 1$)

For class Ib equation (2.12) becomes

$$[(p+\alpha)^2 + (q+\beta)^2]^{\frac{1}{4}} + [(p-\alpha)^2 + (q-\beta)^2]^{\frac{1}{4}} = 2. \tag{2.14}$$

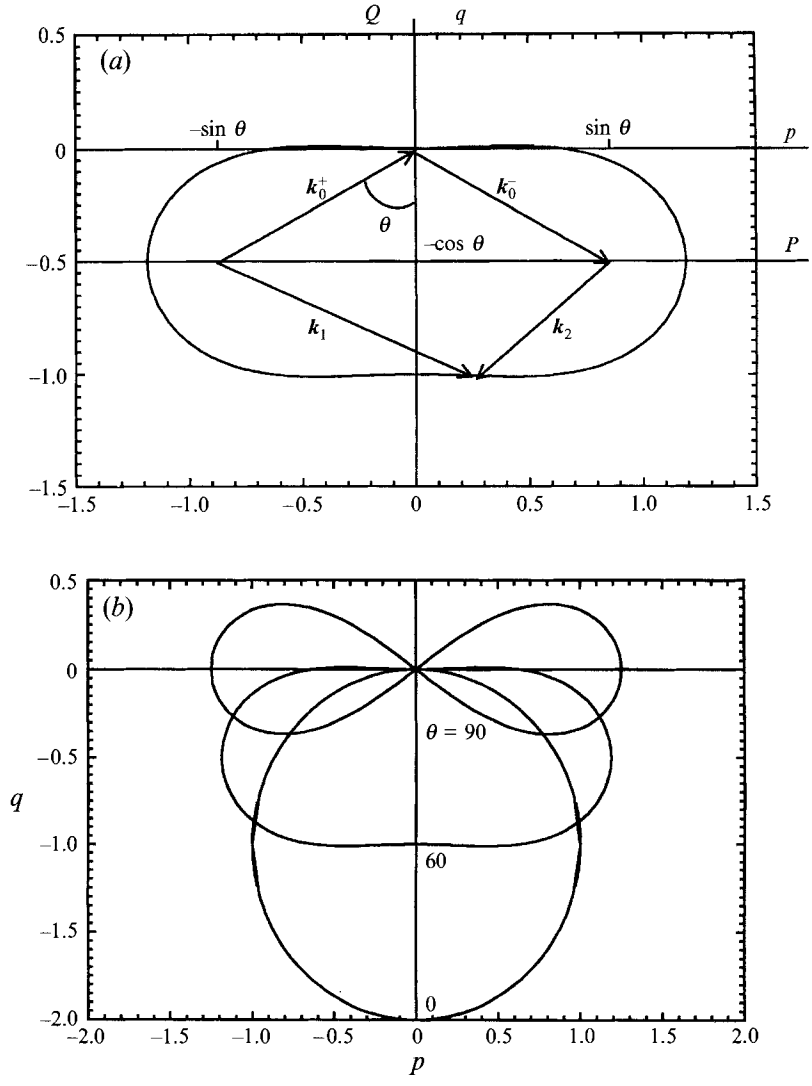

FIGURE 2. (*a*) Resonance curves of class Ia ($j = 1, K_1 = K_2 = 1$) from the linear dispersion relation. (*b*) Resonance curves for various values of the angle θ.

Using $P = p\alpha + q\beta$ and $Q = -p\beta + q\alpha$ the dispersion relation is transformed into

$$[(P+1)^2+Q^2]^{\frac{1}{4}}+[(P-1)^2+Q^2]^{\frac{1}{4}} = 2.$$

The resonance curve is symmetrical about the P-axis and the Q-axis. Following the same procedure previously described we have

$$\boldsymbol{k}_1 = \boldsymbol{k}_2 + 2\boldsymbol{k}_{01},$$
$$\omega_1' = \omega_2' + 2\omega_0',$$

and

$$\boldsymbol{k}_1 = (p+\alpha, q+\beta)^t, \quad \boldsymbol{k}_2 = (p-\alpha, q-\beta)^t, \quad \boldsymbol{k}_{01} = \boldsymbol{k}_0^+ = (\alpha, \beta)^t,$$
$$\omega_1' = |\boldsymbol{k}_1|^{\frac{1}{2}}, \quad \omega_2' = -|\boldsymbol{k}_2|^{\frac{1}{2}}, \quad \omega_0' = 1.$$

Figure 3(*a*) exhibits the corresponding geometrical construction and in figure 3(*b*) are plotted the resonance curves for different values of θ. Class Ib′ and class Ib are

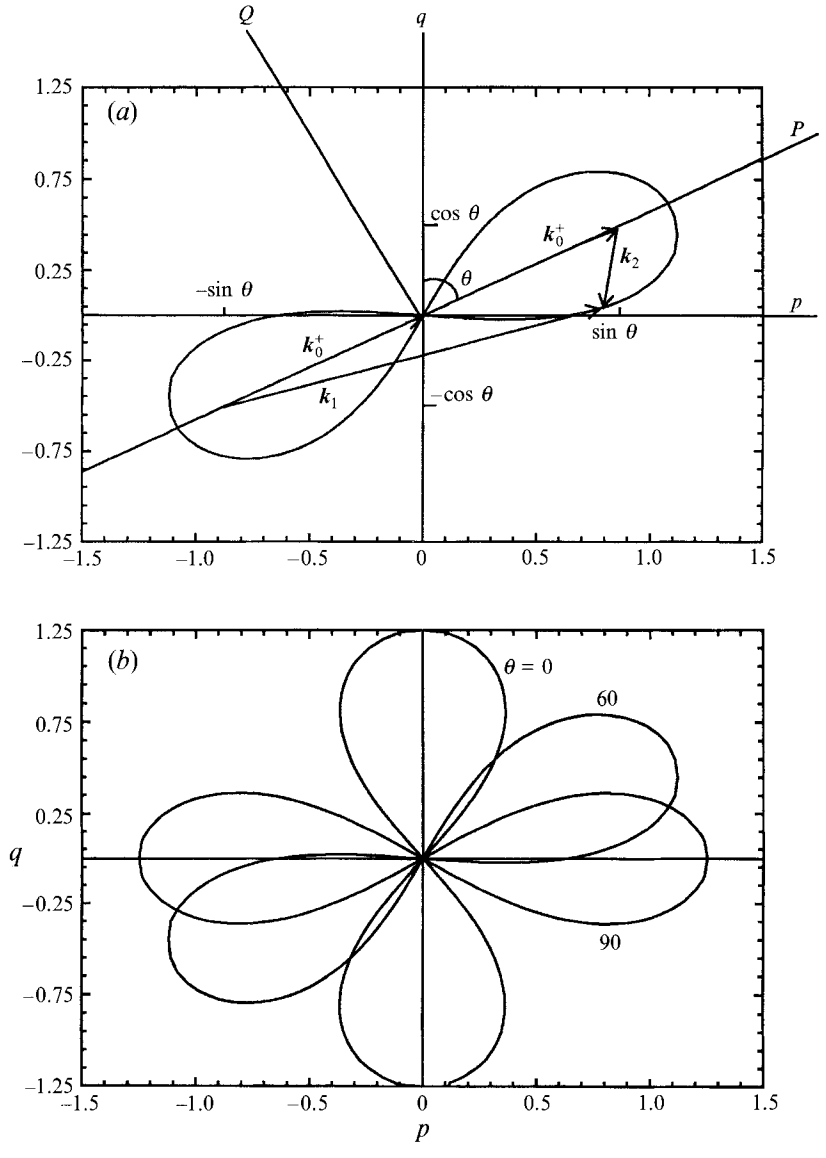

FIGURE 3. Same as figure 2, for class Ib ($j = 1, K_1 = 1, K_2 = -1$).

symmetrical about the p-axis. Note that classes Ia, Ia′, Ib, Ib′ are identical for $\theta = 90°$. For given values of p and q instabilities of class Ia and class Ib (respectively class Ia′ and class Ib′) cannot appear simultaneously.

Class IIa ($j = 1, K_1 = 1, K_2 = 2$) *or class IIa′* ($j = 1, K_1 = -1, K_2 = -2$)

For class IIa the resonance condition (2.12) is

$$[(p+\alpha)^2+(q+\beta)^2]^{\frac{1}{4}}+[(p-2\alpha)^2+(q+2\beta)^2]^{\frac{1}{4}} = 3. \tag{2.15}$$

Using the transformation

$$P = (p\alpha-\tfrac{1}{3}q\beta-\tfrac{4}{9}\beta^2)/(1-\tfrac{8}{9}\beta^2) \quad \text{and} \quad Q = (-q\alpha+\tfrac{1}{8}p\beta-\tfrac{4}{3}\alpha\beta)/(1-\tfrac{8}{9}\beta^2)$$

(2.15) may be written

$$[(P+1)^2+Q^2]^{\frac{1}{4}}+[(P-2)^2+Q^2]^{\frac{1}{4}} = 3/((1-\tfrac{1}{8}\beta^2)^{\frac{1}{4}}).$$

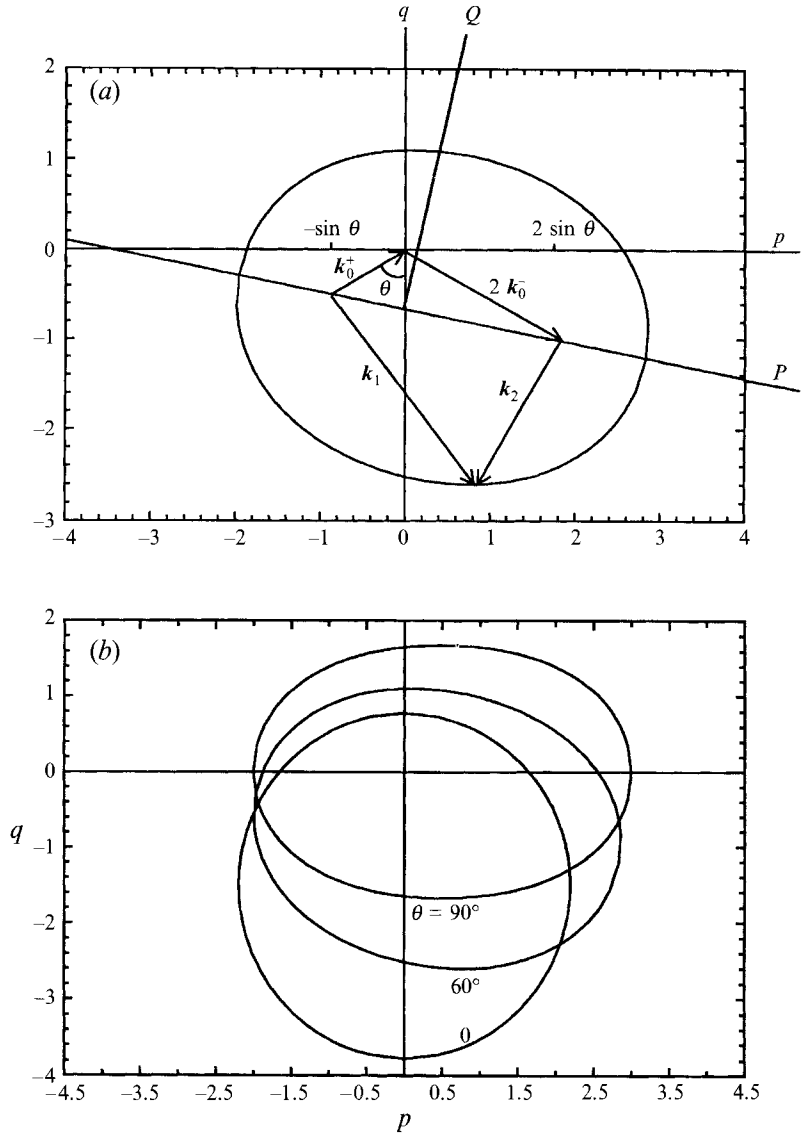

FIGURE 4. Same as figure 2, for class IIa ($j = 1, K_1 = 1, K_2 = 2$).

The resonance curve is symmetrical about the P-axis. Figure 4(a) shows the geometrical construction of the resonance while figure 4(b) displays resonances curves for a set of angles θ:

$$\boldsymbol{k}_1 = \boldsymbol{k}_2 + \boldsymbol{k}_{01} + 2\boldsymbol{k}_{02},$$
$$\omega_1' = \omega_2' + 3\omega_0',$$

and

$$\boldsymbol{k}_1 = (p+\alpha, q+\beta)^t, \quad \boldsymbol{k}_2 = (p-2\alpha, q+2\beta)^t,$$
$$\boldsymbol{k}_{01} = \boldsymbol{k}_0^+ = (\alpha, \beta)^t, \quad \boldsymbol{k}_{02} = \boldsymbol{k}_0^- = (\alpha, -\beta)^t,$$
$$\omega_1' = |\boldsymbol{k}_1|^{\frac{1}{2}}, \quad \omega_2' = -|\boldsymbol{k}_2|^{\frac{1}{2}}, \quad \omega_0' = 1.$$

Resonance curves corresponding, respectively, to class IIa and class IIa′ are symmetrical, about the p-axis. The case of $\theta = 90°$ corresponds to McLean's class II ($N = 3$).

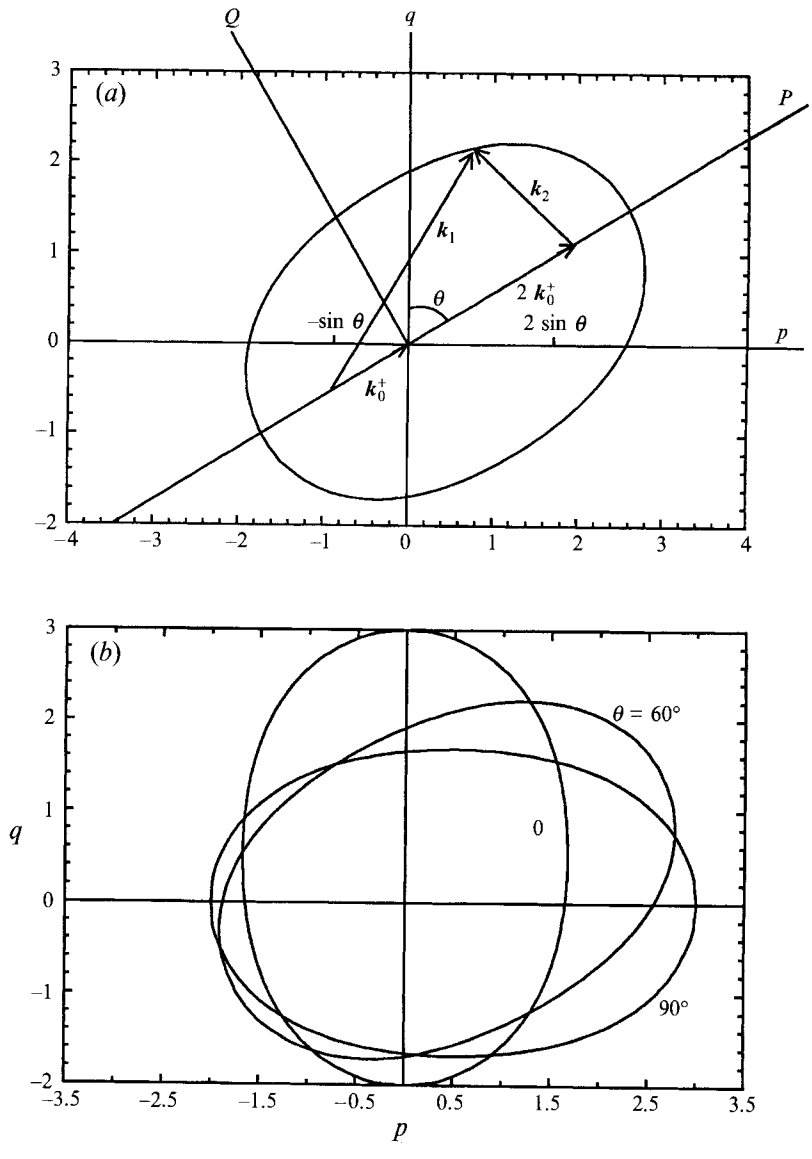

FIGURE 5. Same as figure 2, for class IIb ($j = 1, K_1 = 1, K_2 = -2$).

Class IIb ($j = 1, K_1 = 1, K_2 = -2$) *or class IIb′* ($j = 1, K_1 = -1, K_2 = 2$)

For class IIb, equation (2.12) may be written in the form

$$[(p+\alpha)^2+(q+\beta)^2]^{\frac{1}{4}}+[(p-2\alpha)^2+(q-2\beta)^2]^{\frac{1}{4}} = 3. \tag{2.16}$$

Using $P = p\alpha+q\beta$ and $Q = -p\beta+q\alpha$, equation (2.16) becomes

$$[(P+1)^2+Q^2]^{\frac{1}{4}}+[(P-2)^2+Q^2]^{\frac{1}{4}} = 3.$$

The resonance curve is symmetrical about the P-axis. Figures 5(*a*) and 5(*b*) correspond to this case for different angles θ with

$$\boldsymbol{k}_1 = \boldsymbol{k}_2+3\boldsymbol{k}_{01},$$
$$\omega_1' = \omega_2'+3\omega_0',$$

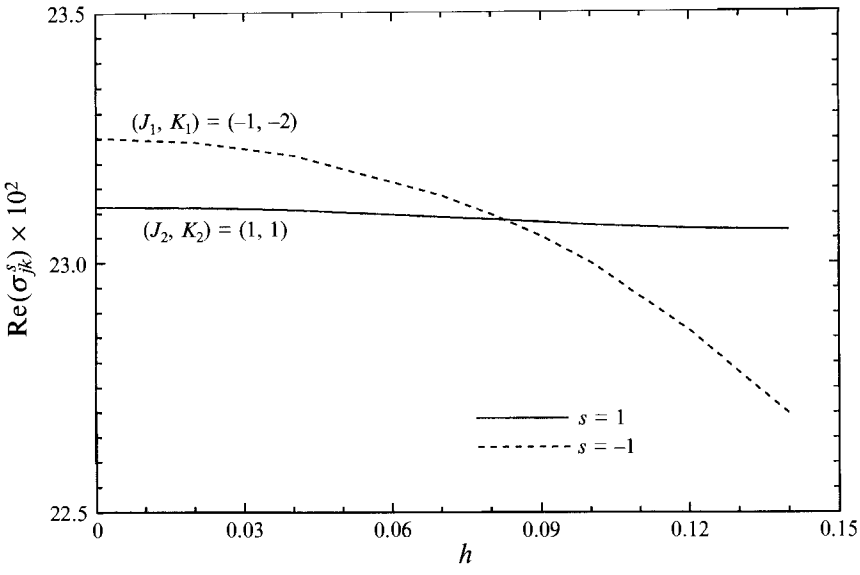

FIGURE 6. Crossing of two eigenvalues of different signatures without the emergence of instability.

and $$\boldsymbol{k}_1 = (p+\alpha, q+\beta)^t, \quad \boldsymbol{k}_2 = (p-2\alpha, q-2\beta)^t, \quad \boldsymbol{k}_{01} = \boldsymbol{k}_0^+ = (\alpha, \beta)^t,$$
$$\omega_1' = |\boldsymbol{k}_1|^{\frac{1}{2}}, \quad \omega_2' = -|\boldsymbol{k}_2|^{\frac{1}{2}}, \quad \omega_0' = 1.$$

Herein also stability diagrams of class II b′ are symmetrical with diagrams of class II b relatively to the p-axis. Classes II a, II a′, II b, II b′ are identical for $\theta = 90°$. Class II interactions require one more fundamental wave vector for the basic wave than class I interactions and therefore are of higher order.

Note that the harmonics of the basic wave which give rise to the instability must exhibit symmetry with respect to a reflection. Figure 6 describes a crossing of two eigenvalues of different signatures without any loss of stability. In that particular case the basic wave does not contain the harmonic $(1, 2)$ which would allow an instability of class I$(j = 1, K_1 = 1, K_2 = -2)$ to appear.

Instabilities for which corresponding eigenvectors have dominant components $a_{J_1K_1}$, $a_{J_2K_2}$, $b_{J_1K_1}$ and $b_{J_2K_2}$ will be identified as class (J_1, J_2, K_1, K_2) instabilities. The instabilities are detected by investigating the vicinity of the linear resonance curves in the (p, q)-plane for $h > 0$.

Let us illustrate briefly the superharmonic case, i.e. $p = q = 0$, previously studied by Ioualalen & Kharif (1993). The authors identified harmonic resonances described by Roberts (1983) as superharmonic instabilities of class I. Roberts (1983) showed the occurrence of a doubly infinite family of harmonic resonances for critical angles θ_c densely distributed on the θ-interval $[0°, 90°]$. The equation relating the angle θ_c to the (m, n)th harmonic with which resonance may occur is given by

$$\cos^2\theta_c = \frac{m^4 - m^2}{n^2 - m^2}.$$

For example when $(m, n) = (2, 6)$ the critical angle $\theta_c = 52°.23\ldots$ Ioualalen & Kharif (1993) showed from a stability analysis point of view that the two eigenvalues, corresponding, respectively, to $(+2, 6)$ and $(-2, 6)$ modes, coalesce generating an

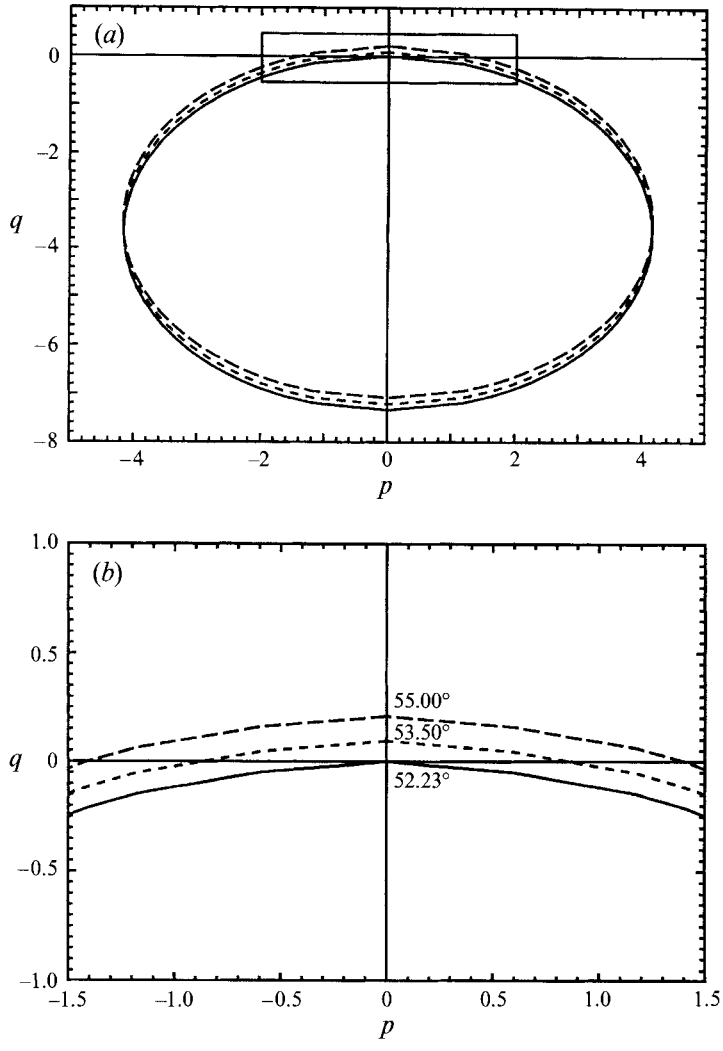

FIGURE 7. (*a*) Resonance curves of class Ia ($j = 2, K_1 = K_2 = 6$) from the linear dispersion relation for angles $\theta = 52°.23$ (——), $\theta = 53°.5$ (- - -), $\theta = 55°$ (– – –). (*b*) An amplification of the curves near the origin $(p, q) = (0, 0)$.

instability of class I($j = 2, K_1 = K_2 = 6$) for $h \geqslant 0$. For $h = 0$ the resonance condition is

$$[(p+2\alpha)^2+(q+6\beta)^2]^{\frac{1}{4}}+[(p-2\alpha)^2+(q-6\beta)^2]^{\frac{1}{4}} = 4.$$

Resonance curves in the (p, q)-plane are shown in figure 7 for different angles θ. The curve for $\theta = 52°.23$ crosses the origin $(p, q) = (0, 0)$ which corresponds to an instability with zero frequency as shown by the authors.

3. Numerical schemes

In this section indices (j, k) will be used instead of (J, K). The series (2.11) are truncated with j and k up to the orders M and N, respectively, and substituted into (2.9) and (2.10), which leads to the following eigenvalue problem for σ with eigenvector $\boldsymbol{u} = (a_{jk}, b_{jk})^t$:

$$\boldsymbol{A}\boldsymbol{u} = \mathrm{i}\sigma\boldsymbol{B}\boldsymbol{u}.$$

	$h = 0.10$		$h = 0.20$		Time CPU
$M = N$	$\mathrm{Im}(\sigma)$	$-\mathrm{Re}(\sigma)$	$\mathrm{Im}(\sigma)$	$-\mathrm{Re}(\sigma)$	(s)
2	0.2667558643(−02)	0.4612204728(−01)			
3	0.1174960579(−02)	0.4540438254(−01)			
4	0.1179979978(−02)	0.4540342927(−01)	0.3516755(−02)	0.4294063(−01)	5.3
5	0.1179888091(−02)	0.4540325445(−01)	0.2894755(−02)	0.4323800(−01)	13.7
6	0.1179889936(−02)	0.4540325698(−01)	0.2963601(−02)	0.4326600(−01)	35.9
7	0.1179889837(−02)	0.4540325688(−01)	0.2949847(−02)	0.4326989(−01)	77.7
8	0.1179889840(−02)	0.4540325689(−01)	0.2944620(−02)	0.4326811(−01)	161.6
9	0.1179889840(−02)	0.4540325689(−01)	0.2951998(−02)	0.4327083(−01)	316.6

TABLE 1. Examples of the dependence of the eigenvalues on the truncation $p = 0.10$, $q = 0.075$ and $\theta = 80°$ (collocation method)

Here $\boldsymbol{A}$ and $\boldsymbol{B}$ are complex matrices depending on the basic wave and the real wavenumbers p and q. Two numerical solution methods have been used and compared: (*a*) a collocation method developed by McLean (1982) to study the linear stability of Stokes waves and (*b*) a Galerkin method developed by Zhang & Melville (1987) to study the linear stability of gravity–capillary waves. Ioualalen & Kharif (1993) extended both methods to the three-dimensional stability analysis and established that the Galerkin method is more efficient. Using a Galerkin method for short-crested nonlinear waves they obtained values for the relevant eigenvalues with two or three more significant figures than those obtained using a collocation method for M, N given and h greater than 0.19; here, both methods are used to treat subharmonic perturbations. The computational efficiencies of the two methods are compared.

3.1. *Collocation method*

This method consists in satisfying the system of equations (2.9) and (2.10) at $(2M+1)(2N+1)$ collocation points distributed over one period of the free surface in the two horizontal directions x and y. We obtain the following equations:

$$\sum_{j=-M}^{M}\sum_{k=-N}^{N} R_{jk}^{(1)} a_{jk} + \sum_{j=-M}^{M}\sum_{k=-N}^{N} S_{jk}^{(1)} b_{jk} = \mathrm{i}\sigma \sum_{j=-M}^{M}\sum_{k=-N}^{N} T_{jk}^{(1)} a_{jk}, \tag{3.1}$$

$$\sum_{j=-M}^{M}\sum_{k=-N}^{N} R_{jk}^{(2)} a_{jk} + \sum_{j=-M}^{M}\sum_{k=-N}^{N} S_{jk}^{(2)} b_{jk} = \mathrm{i}\sigma \sum_{j=-M}^{M}\sum_{k=-N}^{N} T_{jk}^{(2)} b_{jk}, \tag{3.2}$$

where

$$R_{jk}^{(1)} = [-\bar{\phi}_{zz} + \mathrm{i}(p+j\alpha)\bar{\phi}_x + \mathrm{i}(q+k\beta)\bar{\phi}_y + \bar{\eta}_x\bar{\phi}_{xz} + \bar{\eta}_y\bar{\phi}_{yz}]\,\mathrm{e}^{\mathrm{i}(j\alpha x+k\beta y)}, \tag{3.3a}$$

$$S_{jk}^{(1)} = [\mathrm{i}(p+j\alpha)\bar{\eta}_x + \mathrm{i}(q+k\beta)\bar{\eta}_y - \kappa_{jk}]\,\mathrm{e}^{\mathrm{i}(j\alpha x+k\beta y)}\,\mathrm{e}^{\kappa_{jk}\bar{\eta}}, \tag{3.3b}$$

$$T_{jk}^{(1)} = \mathrm{e}^{\mathrm{i}(j\alpha x+k\beta y)}, \tag{3.3c}$$

$$R_{jk}^{(2)} = (1 + \bar{\phi}_x\bar{\phi}_{xz} + \bar{\phi}_y\bar{\phi}_{yz} + \bar{\phi}_z\bar{\phi}_{zz})\,\mathrm{e}^{\mathrm{i}(j\alpha x+k\beta y)}, \tag{3.3d}$$

$$S_{jk}^{(2)} = [\mathrm{i}(p+j\alpha)\bar{\phi}_x + \mathrm{i}(q+k\beta)\bar{\phi}_y + \kappa_{jk}\bar{\phi}_z]\,\mathrm{e}^{\mathrm{i}(j\alpha x+k\beta y)}\,\mathrm{e}^{\kappa_{jk}\bar{\eta}}, \tag{3.3e}$$

$$T_{jk}^{(2)} = \mathrm{e}^{\mathrm{i}(j\alpha x+k\beta y)}\,\mathrm{e}^{\kappa_{jk}\bar{\eta}}. \tag{3.3f}$$

A standard eigenvalue solver (QZ algorithm) is used to find the $2(2M+1)(2N+1)$ eigenvalues of the system (3.1)–(3.2). The integers M and N are increased until the eigenvalues σ have converged. Table 1 shows examples of eigenvalue convergence for two different values of the wave steepness of the basic wave. The last column

gives the CPU calculation time on a CRAY II computer, proportional to L^3 with $L = 2(2M+1)(2N+1)$. This table reveals that as the wave steepness increases, the method yields less accurate results. To improve the accuracy it is necessary to increase the number of collocation points, and thus the order of the matrices $\boldsymbol{A}$ and $\boldsymbol{B}$ may become too large to treat the eigenvalue problem accurately. The limitation of this method for highly nonlinear short-crested waves is due to the fact that the number of modes in the truncated eigenvectors is fixed equal to the number of discrete points on the free surface. In this way the effects of these two numbers on the convergence are treated equally. Consequently either the number of modes may be much larger than necessary for a given accuracy or the number of collocation points may be insufficient to correctly describe the free surface. A Galerkin method has been used in order to dissociate the effect of the two numbers.

3.2. *Galerkin method*

Zhang & Melville (1987) pointed out that the number of modes required for a sufficient accuracy using a Galerkin method is less than the number of collocation points, i.e. the corresponding number of modes in the collocation method. The main advantage of this method is the generality allowed in the spectral representation of the surface. The method developed by Zhang & Melville (1987) is extended to the case of a three-dimensional basic wave. Applying Fourier transforms to (3.1) and (3.2) and approximating integrals on a grid of $\nu \times \mu$ points, the coordinates of which are

$$x_u = \frac{2\pi u}{\alpha \nu}, \quad u = 0, \ldots, \nu - 1,$$

$$y_v = \frac{2\pi v}{\beta \mu}, \quad v = 0, \ldots, \mu - 1,$$

we obtain the following system after exchanging the orders of summation (j,k) and (u,v):

$$\sum_{j=-M}^{M} \sum_{k=-N}^{N} F_{j-l,k-r}\{E_{jk}^{(1)}\} a_{jk} + \sum_{j=-M}^{M} \sum_{k=-N}^{N} F_{j-l,k-r}\{G_{jk}^{(1)}\} b_{jk} = \mathrm{i}\sigma a_{ir}, \tag{3.4}$$

$$\sum_{j=-M}^{M} \sum_{k=-N}^{N} F_{j-l,k-r}\{E_{jk}^{(2)}\} a_{jk} + \sum_{j=-M}^{M} \sum_{k=-N}^{N} F_{j-l,k-r}\{G_{jk}^{(2)}\} b_{jk} = \mathrm{i}\sigma \sum_{j=-M}^{M} \sum_{k=-N}^{N} F_{j-l,k-r}\{H_{jk}\} b_{jk}, \tag{3.5}$$

where

$$E_{jk}^{(i)} = R_{jk}^{(i)}/T_{jk}^{(1)}, \quad i = 1,2,$$

$$G_{jk}^{(i)} = S_{jk}^{(i)}/T_{jk}^{(1)}, \quad i = 1,2,$$

$$H_{jk} = T_{jk}^{(2)}/T_{jk}^{(1)}.$$

The functions

$$F_{j-l,k-r}\{f_{jk}\} = \sum_{u=0}^{\nu-1} \sum_{v=0}^{\mu-1} f_{jk}\, \mathrm{e}^{\mathrm{i}\alpha(j-l)x_u}\, \mathrm{e}^{\mathrm{i}\beta(k-r)y_v},$$

where $l = -M, \ldots, M$ and $r = -N, \ldots, N$ are computed using two-dimensional fast Fourier transforms (FFT). The weak constraints to be satisfied are $M < \frac{1}{2}\nu$ and $N < \frac{1}{2}\mu$. An eigenvalue problem is also derived from (3.4) and (3.5). For a given value of the wave steepness h and a fixed value of the angle θ, the integers ν and μ are increased until the Fourier coefficients have converged. The convergence of the eigenvalues is obtained by increasing M and N. Generally, the number of discrete points required to describe the free surface is much larger than the number of modes

(ν, μ)	$\mathrm{Re}(F_{-2,-2})$	$\mathrm{Im}(F_{-2,-2})$
(10, 10)	0.2657612477(−02)	0.4349091737(−01)
(12, 12)	0.2850392756(−02)	0.4336533422(−01)
(15, 15)	0.2840724011(−02)	0.4337641063(−01)
(18, 18)	0.2840717591(−02)	0.4337640590(−01)
(20, 20)	0.2840723404(−02)	0.4337641234(−01)
(25, 25)	0.2840723271(−02)	0.4337641093(−01)
(30, 30)	0.2840723272(−02)	0.4337641093(−01)
(60, 60)	0.2840723271(−02)	0.4337641093(−01)

TABLE 2. Convergence of the $F_{-2,-2}$ coefficient for $h = 0.20$, $\theta = 80°$, $p = 0.10$ and $q = 0.075$

	$h = 0.10$		$h = 0.20$		
$M = N$	$\mathrm{Im}(\sigma)$	$-\mathrm{Re}(\sigma)$	$\mathrm{Im}(\sigma)$	$-\mathrm{Re}(\sigma)$	Time CPU (s)
2	0.1128301558(−02)	0.4543339417(−01)	0.5273342(−02)	0.4971916(−01)	2.8
3	0.1179391342(−02)	0.4540385737(−01)	0.2779965(−02)	0.4341529(−01)	3.9
4	0.1179779460(−02)	0.4540349248(−01)	0.2840723(−02)	0.4337641(−01)	9.2
5	0.1179888153(−02)	0.4540325936(−01)	0.2944414(−02)	0.4327712(−01)	16.1
6	0.1179889672(−02)	0.4540325741(−01)	0.2949270(−02)	0.4327394(−01)	38.6
7	0.1179889836(−02)	0.4540325689(−01)	0.2951651(−02)	0.4327102(−01)	85.7
8	0.1179889839(−02)	0.4540325689(−01)	0.2951841(−02)	0.4327084(−01)	170.8
9	0.1179889841(−02)	0.4540325689(−01)	0.2951882(−02)	0.4327078(−01)	334.7

TABLE 3. Examples of the dependence of the eigenvalues on the truncation $p = 0.10$, $q = 0.075$ and $\theta = 80°$ (Galerkin method)

required for convergence of the eigenvalues, avoiding aliasing errors. Table 2 shows the convergence of the $F_{-2,-2}$ coefficient as a function of the (ν, μ) grid of points. For $h = 0.20$ a relative accuracy of order 10^{-10} with $(\nu, \mu) = (25, 25)$ allows a consistent description of the free surface.

Table 3 which is similar to table 1 shows that both methods are of the same order of accuracy for small wave steepness. However, for higher wave steepness the Galerkin method is more efficient with relative accuracy of order 10^{-3} and 10^{-5} for, respectively, $(M, N) = (5, 5)$ and $(M, N) = (7, 7)$ while the corresponding values are only 10^{-1} and 10^{-3} for the collocation method. Thus, the Galerkin method has been retained herein for further calculations.

4. Numerical results

The instability regions corresponding to the two classes I previously described are plotted in figures 8 and 9 for, respectively, $\theta = 80°$, $h = \{0.10, 0.20\}$ and $\theta = 60°$, $h = \{0.10, 0.20\}$. For a fixed value of θ the unstable regions of class Ib grow as the wave steepness increases. Class Ia exhibits similar behaviour except for values of the parameter θ near 60° where the unstable region shrinks dramatically.

In figure 8 the dominant instability belongs to class Ia with $p \neq N\alpha$ and $q = 0$ while in figure 9(*b*) the dominant instability belongs to class Ib and is located on the axis of symmetry $q = p/\tan\theta$ with $p \neq N\alpha$ and $q \neq M\beta$. From these two examples we observe that the most unstable disturbance of classes Ia, a′ is subharmonic in the x-direction and superharmonic in the y-direction: the most unstable disturbance of classes Ib, b′ is subharmonic in the two orthogonal directions.

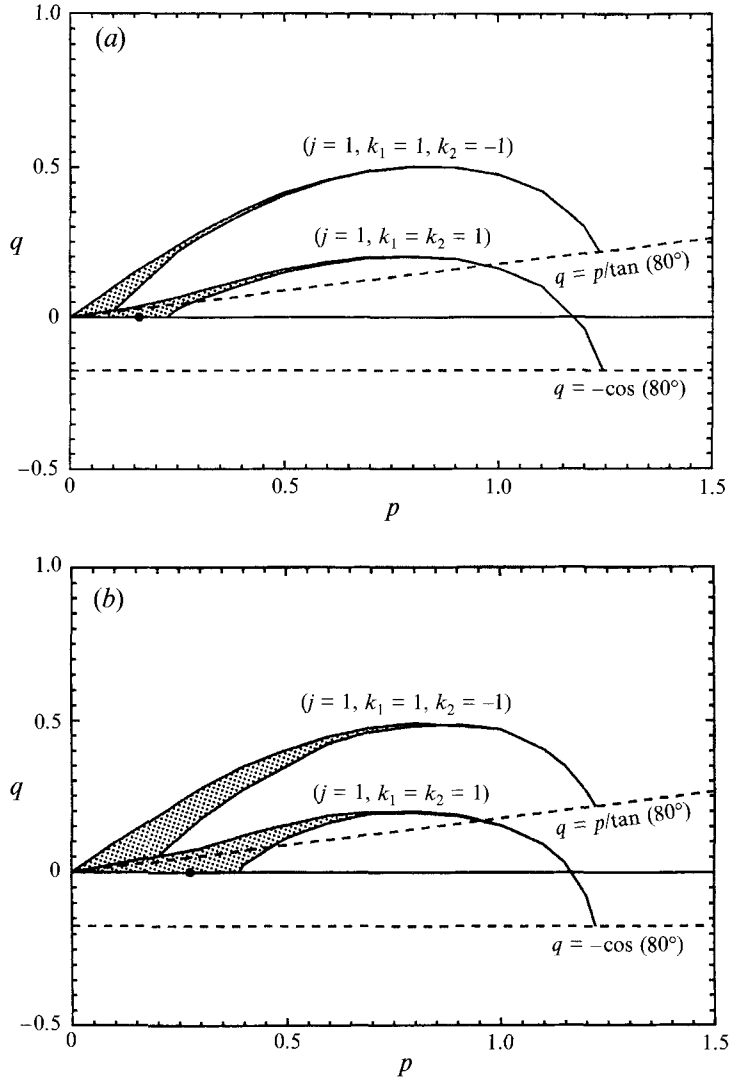

FIGURE 8. Instability regions of class I for $\theta = 80°$. The labelled dots correspond to the maximum growth rate of the instability. (*a*) $h = 0.10$, (*b*) $h = 0.20$.

In figure 10 are plotted the maximum growth rates of classes I as a function of the angle θ for different values of the wave steepness h. Instabilities of class Ia are similar to the Benjamin–Feir modulational perturbations in the x-direction. At $\theta = 90°$, their rates of growth for small amplitudes are of order $(h/\pi)^2$ and decrease rapidly as θ decreases to become very weak near $\theta = 55°$.† A restabilization of instabilities of this class may occur for steep three-dimensional gravity waves but these are beyond the scope of our study. Kharif & Ramamonjiarisoa (1988) showed that class I($m = 1$) instabilities of Stokes waves ($\theta = 90°$) disappear for the wave of maximum energy. The maximum growth rates of instabilities of Stokes waves ($\theta = 90°$) for $h = 0.10$ and 0.20 are respectively 0.4×10^{-2} and 1.33×10^{-2} (see table 2 of McLean 1982). Extension to $h = 0.15$ gives as maximum growth rate 0.83×10^{-2}. These values are markedly higher

† As suggested by a referee, minimum values near $\theta = 55°$ seem to be close to the complement of the angle between groups and waves on the boundary wedge of the Kelvin ship-wave pattern.

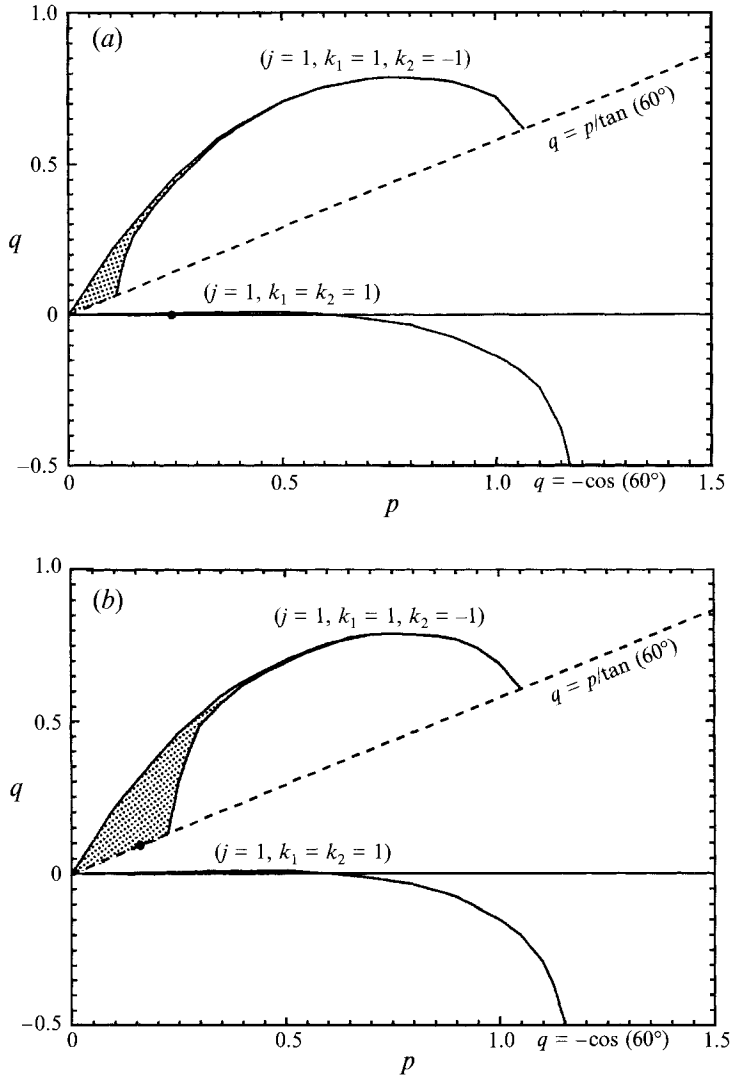

FIGURE 9. Same as figure 8, for $\theta = 60°$.

than one would guess for $\theta = 90°$ from figure 10 and so it is shown that two-dimensional progressive gravity waves are strongly more unstable than fully three-dimensional progressive gravity waves. Near-standing waves which correspond to small values of θ are subject to modulational instabilities of class Ia with rates of growth close to those of long-crested waves (θ close to 90°). Mercer & Roberts (1992) showed that pure standing waves ($\theta = 0°$), which cannot be treated by the present formulation, are unstable to subharmonic perturbations.

Instability regions of classes Ia and Ib associated with long-crested waves intersect near the origin $(p, q) = (0, 0)$. As previously noted these instabilities cannot appear simultaneously at the same point in the (p, q)-plane, which avoids the most unstable perturbation of class Ib being located on the axis of symmetry $q = p \tan\theta$. This explains the gap between the growth rates of instabilities of the two classes for θ near 90°. The resonance curves of classes Ia and Ib become identical for $\theta = 90°$ and $h = 0$. For any given steepness, h, the maximum rate of growth of class Ib remains

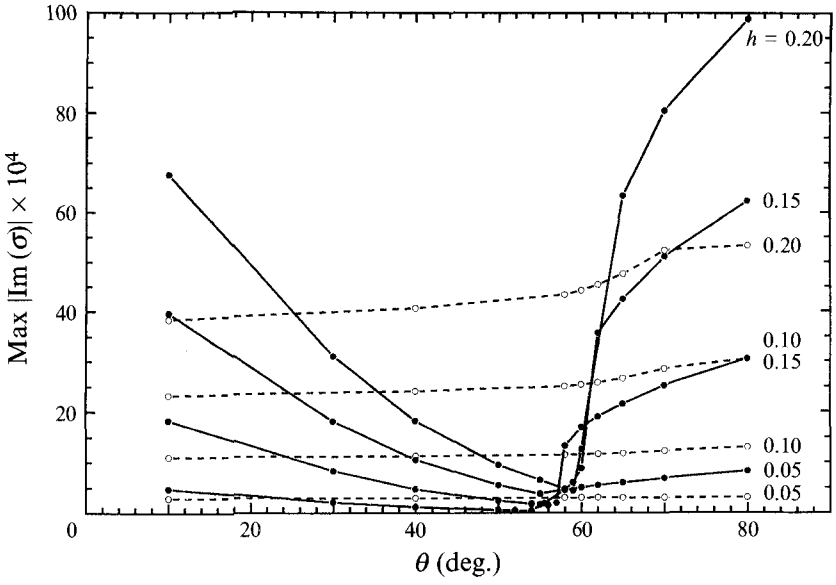

FIGURE 10. Maximum growth rates of class I as a function of the angle θ: —●—, class Ia; --○--, class Ib.

almost constant when θ varies. This is not surprising since this class has linear resonance curves invariant under rotations as shown in figure 3(*b*). In the range defined approximately as $60° < \theta < 90°$ and $\theta < 25°$ the dominant instabilities are of class Ia, subharmonic in the direction of propagation of the basic wave and superharmonic in the transversal direction. Our results are restricted to angles $\theta \neq 0°$ because the present formulation is inadequate to study the linear stability of pure standing waves. In the range $25° < \theta < 60°$ dominant instabilities are of class Ib and are subharmonic in the two horizontal directions. Figure 10 also shows that Stokes waves ($\theta = 90°$), which are two-dimensional, are more unstable than three-dimensional surface gravity waves.

Figures 11 and 12 show wave patterns of undisturbed and disturbed flows corresponding, respectively, to class Ia and class Ib. The perturbed flow is composed of the superposition of the basic wave ($\bar{\eta}(x, y)$ and the perturbation

$$\epsilon \,\mathrm{Re}\{\eta'_{p,q}(x,y) + \eta'_{p,-q}(x,y)\}.$$

Figure 11(*c*) shows that modulation occurs only in the longitudinal direction while figure 12(*c*) reveals modulation in both the longitudinal and transversal directions. Figures 13 and 14 display longitudinal profiles in the plane $y = 0$ and transversal profiles in the plane $x = 0$ for the surface waves shown, respectively, in figures 11 and 12 and illustrate more clearly the modulation phenomenon.

Using a pseudo-spectral method Poitevin & Kharif (1991) computed the nonlinear evolution of a Stokes wave train subject to a sideband-type instability and observed the frequency down-shifting phenomenon when dissipation is taken into account. In order to study subharmonic transitions it would be relevant to extend the direct numerical calculations to three-dimensional deep water waves. These subharmonic transitions would change the angle θ into angle θ'. In this case for classes Ia, a′ the dominant components of unstable modes lead to

$$\theta' = \arctan\frac{\sin\theta - p}{\cos\theta + q} \quad \text{with} \quad q = 0.$$

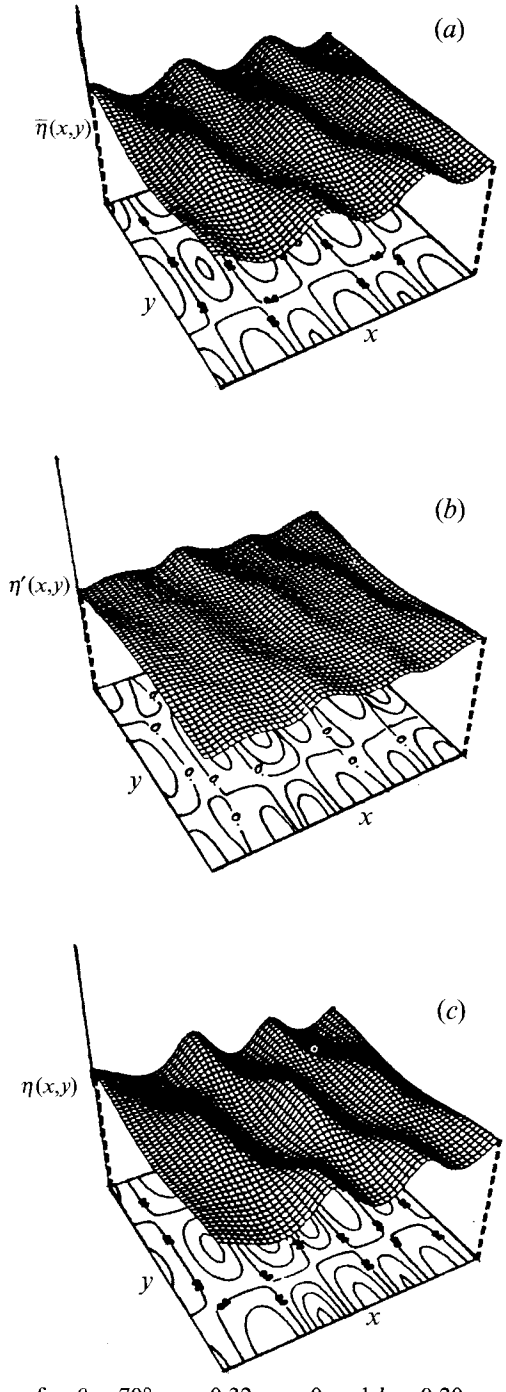

FIGURE 11. Wave pattern for $\theta = 70°$, $p = 0.32$, $q = 0$ and $h = 0.20$ over several periods in the horizontal direction: (*a*) unperturbed wave, (*b*) perturbation ($\epsilon = 0.05$), (*c*) perturbed wave.

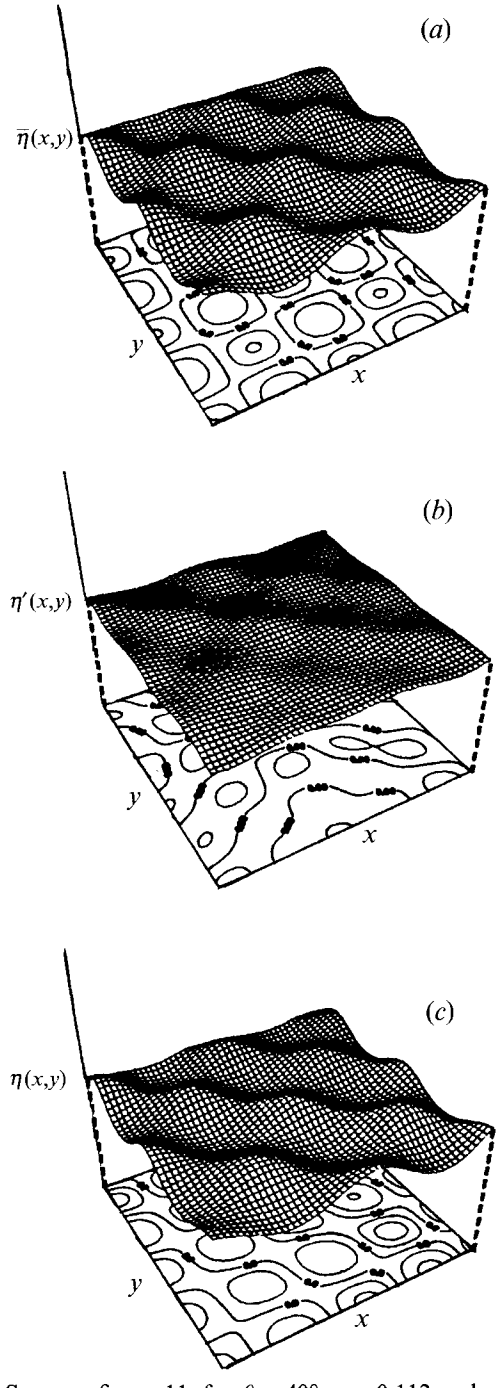

FIGURE 12. Same as figure 11, for $\theta = 40°$, $p = 0.112$ and $q = \pm 0.1335$.

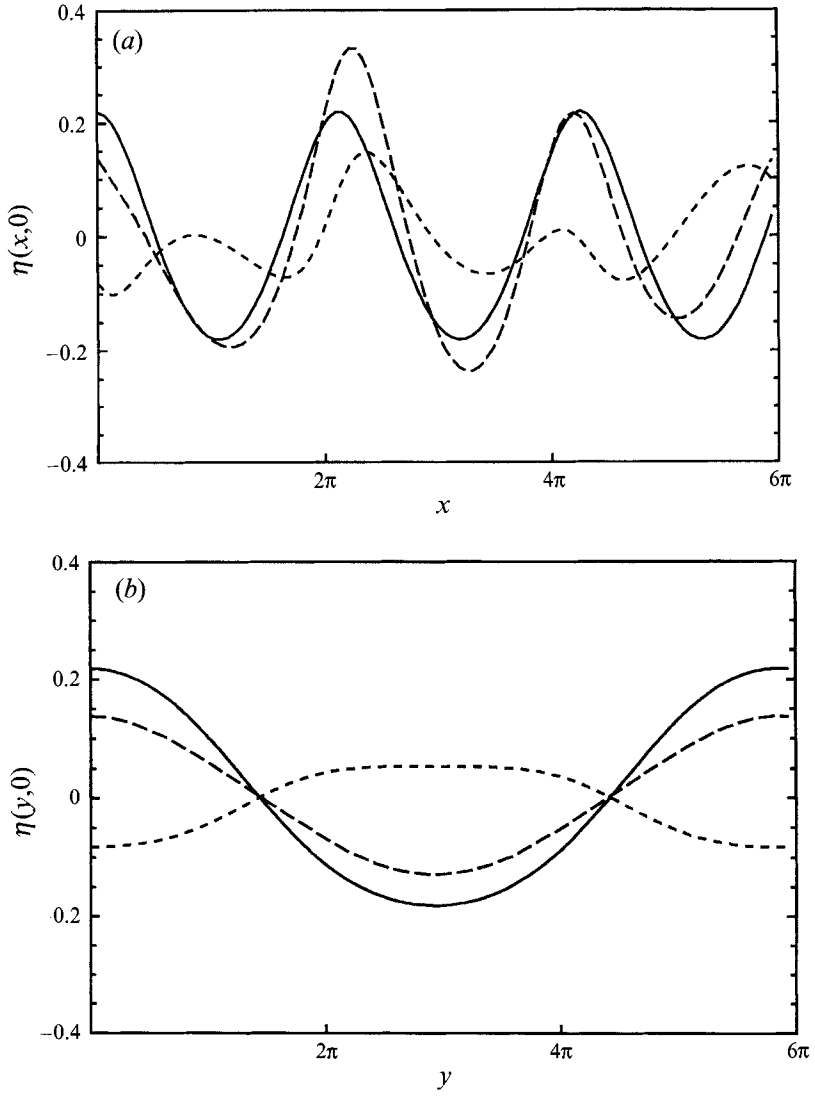

FIGURE 13. Wave pattern for $\theta = 70°$, $p = 0.32$, $q = 0$ and $h = 0.20$: ——, unperturbed wave; - - -, perturbation; — — —, perturbed wave. (*a*) In the plane $y = 0$, (*b*) in the plane $x = 0$.

For classes Ib, b′ the dominant components of the unstable modes lead to

$$\theta' = \arctan\frac{\sin\theta - p}{\cos\theta - q} \quad \text{with} \quad q = p\tan\theta$$

and so $\theta' = \theta$.

For classes Ib, b′, the wavenumbers of the two component waves are down-shifted together so there would be no change in the angle θ of propagation, while for classes Ia, a′ only the longitudinal wavenumber is down-shifted ($q = 0$) so the angle θ would be affected. This means that for $\theta > 45°$ class Ia instabilities would produce three-dimensional wave trains which become more three-dimensional via nonlinear interaction.

Ioualalen & Kharif (1993) investigated numerically the stability of three-dimensional

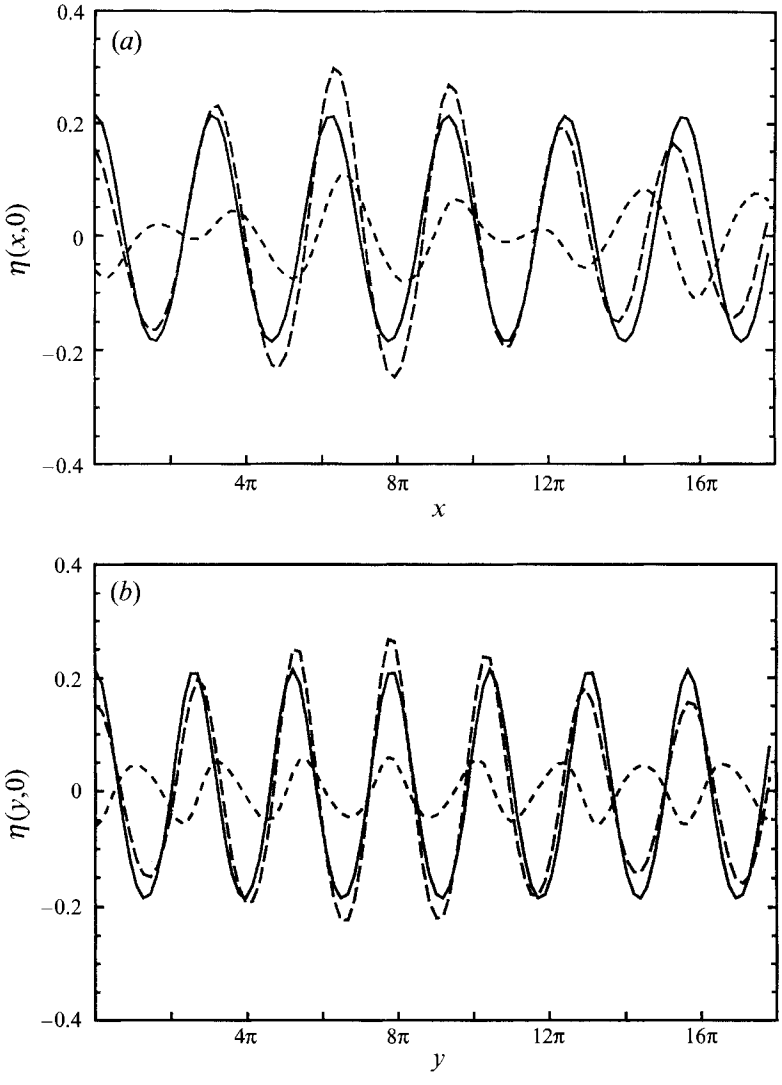

FIGURE 14. Same as figure 13, for $\theta = 40°$, $p = 0.112$ and $q = \pm 0.1335$.

progressive gravity waves on deep water to superharmonic disturbances, also called harmonic resonances. As their main result they showed that these resonances are sporadic 'bubbles' of instabilities which correspond to weak three-dimensional extensions of McLean's class I(m) instabilities for $m \geqslant 2$. They computed the growth rates of different harmonic resonances which never exceed the value $h^{2m}(m \geqslant 2)$ in the range $0.10 \leqslant h \leqslant 0.30$. Herein classes Ia and Ib have been identified as extensions of McLean's class I(m) instabilities for $m = 1$. Thus, the characteristic timescales of harmonic resonances discovered by Roberts (1983) are much greater than those for the subharmonic resonances of modulational type.

The instability regions corresponding to the two classes II defined in §2 are plotted in figures 15 and 16 for, respectively, $\theta = 80°$, $h = \{0.10, 0.20\}$ and $\theta = 60°$, $h = \{0.10, 0.20\}$. These resonances are of higher order than those of classes I and so are weaker for small and moderate values of the wave steepness of the unperturbed wave. The maximum growth rates of classes IIa and IIb are located on their respective axis of

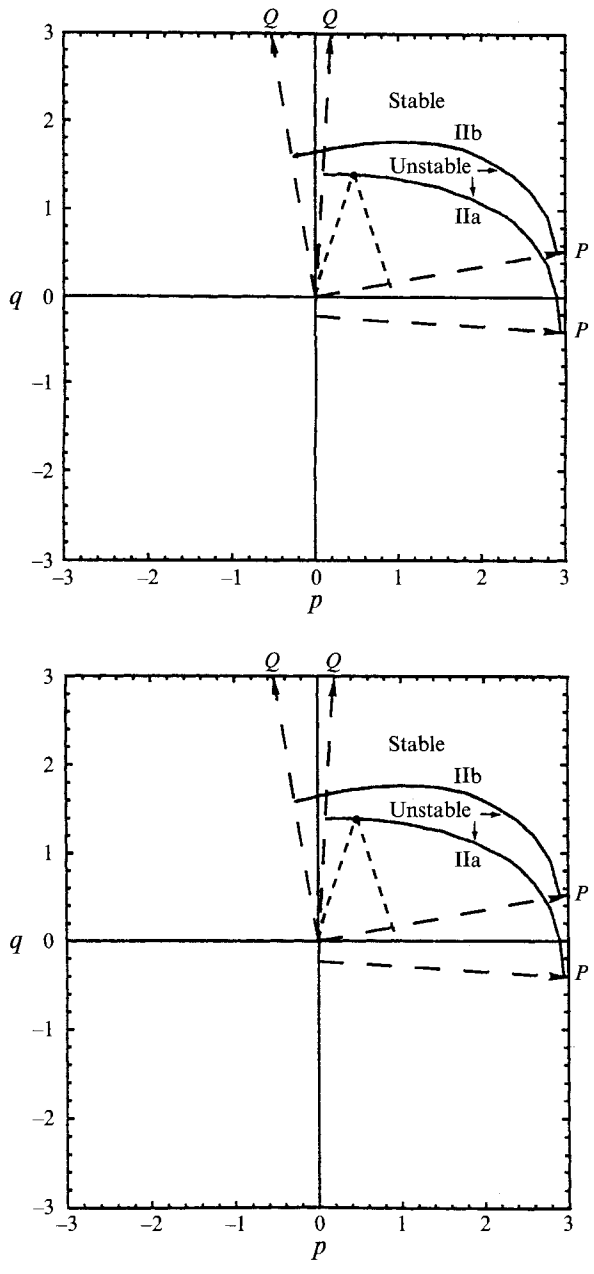

FIGURE 15. Instability regions of class II for $\theta = 80°$. (*a*) $h = 0.10$, (*b*) $h = 0.20$. The dots label the maximum growth rates and the dashed lines correspond to neutral stability.

symmetry $P = \frac{1}{2}$. The dashed lines drawn in the neighbourhood of the stability boundaries of class IIa are points of neutral stability. Generally, the point of maximum instability occurs with $\mathrm{Re}(\sigma) \neq 0$ except for $\theta = 90°$. Therefore, the most unstable perturbation is not phase locked to the unperturbed wave. However the stability boundary at $P = \frac{1}{2}$ may represent a bifurcation of the initial wave pattern. Figures 15 and 16 show that the dominant instabilities for respectively $\theta = 80°$ and $\theta = 60°$ belong to class IIa. Comparison of the growth rates of classes IIa and IIb for $h = 0.10$ and 0.20 as a function of θ is shown in figure 17 and illustrates that class IIa instabilities

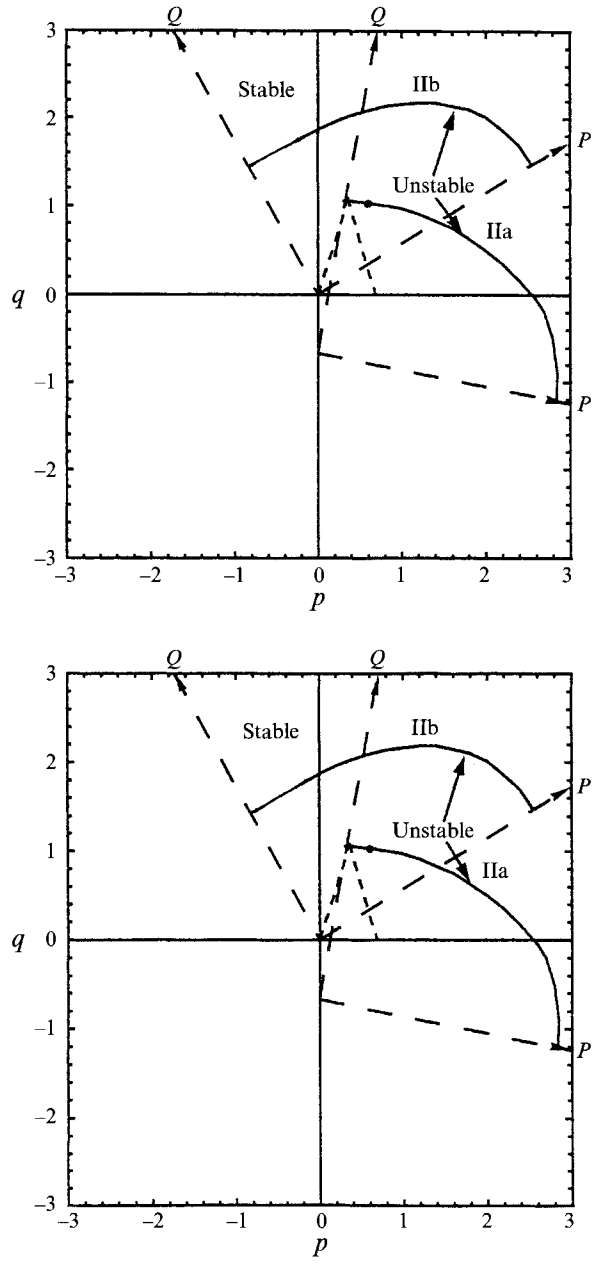

FIGURE 16. Same as figure 15, for $\theta = 60°$.

are dominant in the approximate region $\theta > 55°$. The behaviour of the maximum growth rate of class IIb which remains almost constant when θ varies is similar to that of class Ib.

Figure 18 shows the maximum growth rates of classes I and II for two values, $\theta = 40°$ and $\theta = 80°$. The present computations show that modulational instabilities of class I are predominant over the range $0 \leqslant h \leqslant 0.30$. For $\theta = 80°$ an extrapolation of the curves beyond $h = 0.30$ suggests that class II instabilities would dominate at a critical wave steepness $h_c(\theta)$. The latter is consistent with the results of McLean *et al.* (1981) and McLean (1982) who established that for Stokes waves ($\theta = 90°$) $h_c(\theta) = 0.30$.

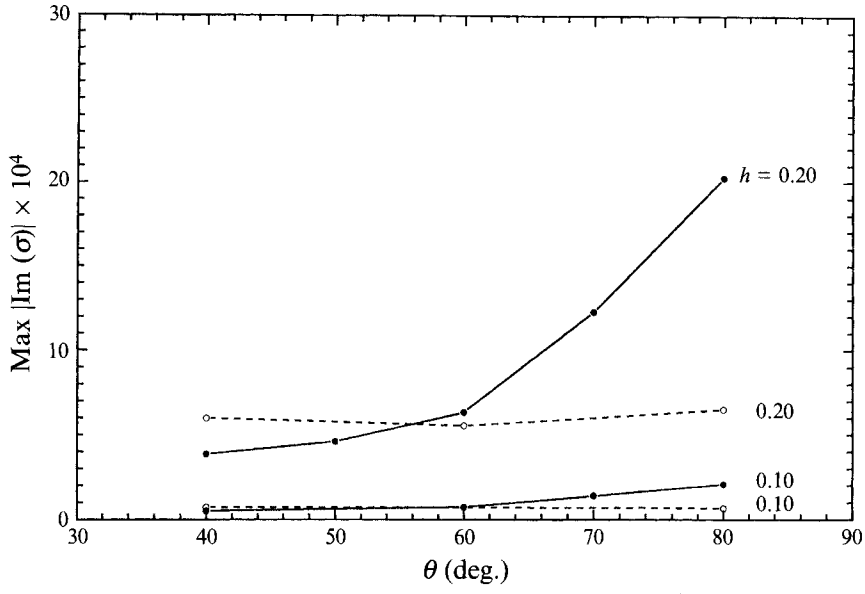

FIGURE 17. Maximum growth rates of class II as a function of the angle θ: ——, class IIa; - - -, class IIb.

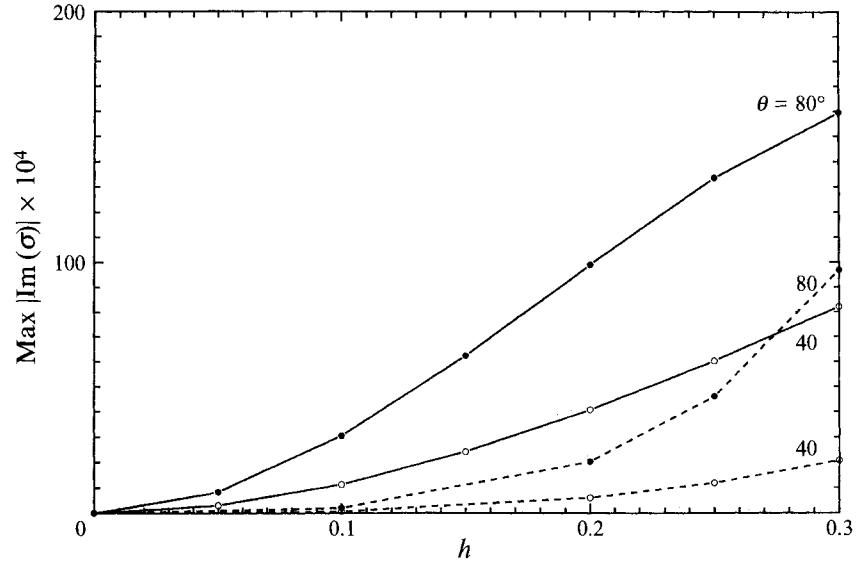

FIGURE 18. Maximum growth rates of dominant instabilities as a function of the wave steepness: —●—, class Ia; —○—, class Ib; --●--, class IIa; --○--, class IIb.

5. Conclusions

The stability analysis presented herein allows the determination of the relevant wave interactions in more realistic water wave fields such as short-crested waves. The mathematical existence of such waves is still an open question. However, useful results have been obtained from approximate solutions via perturbation series and their stability to infinitesimal disturbances. From the latter it has been shown in the range of wave steepness $0 \leqslant h \leqslant 0.30$ that the dominant instabilities are subharmonic in the

direction of propagation of the basic wave and belong to an extension of McLean's class I. Moreover, it is found that the timescales of harmonic resonances given by Ioualalen & Kharif (1993) are much larger than those corresponding to the subharmonic resonances calculated herein; thus harmonic resonances would not have time to develop significantly if compared to subharmonic resonances. It has been also shown that three-dimensional progressive gravity waves are less unstable than two-dimensional progressive gravity waves.

Beyond a wave steepness of $h = 0.30$ the stability computation becomes tedious and thus our analysis has been limited by this value. The numerical scheme presented herein is appropriate for the study of instabilities of classes II which would dominate the resonances occurring in short crested-water waves but further calculations would be necessary since Roberts (1983) showed that the maximum steepness estimates can reach values over 0.7.

The authors wish to thank the CCVR for the computations assistance, and are grateful to B. Garabédian and B. Zucchini for the technical realization of the paper. They also thank the referees and Professors Robert Sani and Eric Mollo-Christensen for improving a first-draft manuscript.

REFERENCES

BENJAMIN, T. B. & FEIR, J. E. 1967 The disintegration of wave trains on deep water. *J. Fluid Mech.* **27**, 417–430.

BRYANT, P. J. 1985 Doubly periodic progressive permanent waves in deep water. *J. Fluid Mech.* **161**, 27–42.

CHAPPELEAR, J. E. 1961 On the description of the short-crested waves. *Beach Erosion Board. US Army Corps Engrs Tech. Memo* no. 125.

FUCHS, R. A. 1952 On the theory of short-crested oscillatory waves. Gravity waves. *US Natl Bur. Stand. Circular* **521**, 187–200.

GILEWICZ, J. 1978 *Approximants de Padé.* Lecture Notes in Mathematics, vol. 667. Springer.

HSU, J. R. C., TSUCHIYA, Y. & SILVESTER, R. 1979 Third-order approximation to short-crested waves. *J. Fluid Mech.* **90**, 179–196.

IOUALALEN, M. 1990 Etude de la stabilité linéaire d'ondes de gravité progressives et tri-dimensionnelles en profondeur infinie. Thèse no. 207.90.76, Univesité Aix-Marseille II.

IOUALALEN, M. 1993 Fourth order approximation of short-crested waves. *C. R. Acad. Sci. Paris* **316** (II), 1193–1200.

IOUALALEN, M. & KHARIF, C. 1993 Stability of three-dimensional progressive gravity waves on deep water to superharmonic disturbances. *Eur. J. Mech.* B/*Fluids* **12**, 401–414.

KHARIF, C. 1987 Etude comparative des instabilités tridimensionnelles et bidimensionnelles des vagues de gravité de forte cambrure. *J. Mech. Theor. Appl.* **3**, 535–550.

KHARIF, C. & RAMAMONJIARISOA, A. 1988 Deep water gravity wave instabilities at large steepness. *Phys. Fluids* **31**, 1286–1288.

KHARIF, C. & RAMAMONJIARISOA, A. 1990 On the stability of gravity waves on deep water. *J. Fluid Mech.* **218**, 163–170.

LONGUET-HIGGINS, M. S. 1978*a* The instabilities of gravity waves of finite amplitude in deep water. I. Superharmonics. *Proc. R. Soc. Lond.* A **360**, 471–488.

LONGUET-HIGGINS, M. S. 1978*b* The instabilities of gravity waves of finite amplitude in deep water. II. Subharmonics. *Proc. R. Soc. Lond.* A **360**, 489–505.

MACKAY, R. S. & SAFFMAN, P. G. 1986 Stability of water waves. *Proc. R. Soc. Lond.* A **406**, 115–125.

MCLEAN, J. W. 1982 Instabilities of finite amplitude water waves. *J. Fluid Mech.* **114**, 315–330.

MCLEAN, J. W., MA, Y. C., MARTIN, D. V., SAFFMAN, P. G. & YUEN, H. C. 1981 Three-dimensional instability of finite amplitude water waves. *Phys. Rev. Lett.* **46**, 817–820.

MERCER, G. N. & ROBERTS, A. J. 1992 Standing waves in deep water. Their stability and extreme form. *Phys. Fluids* A **4**, 259–269.

OKAMURA, M. 1984 Instabilities of weakly nonlinear standing gravity waves. *J. Phys. Soc. Japan* **53**, 3788–3796.

OKAMURA, M. 1986 Maximum wave steepness and instabilities of finite-amplitude standing gravity waves. *Fluid Dyn. Res.* **1**, 201–214.

PHILLIPS, O. M. 1960 On the dynamics of unsteady gravity waves of finite amplitude. *J. Fluid Mech.* **9**, 193–217.

POITEVIN, J. & KHARIF, C. 1991 Subharmonic transition of a nonlinear wave train on deep water. In *Mathematical and Numerical Aspects of Wave Propagation Phenomena*. Philadelphia: SIAM.

ROBERTS, A. J. 1983 Highly nonlinear short-crested water waves. *J. Fluid Mech.* **135**, 301–321.

ROBERTS, A. J. & PEREGRINE, D. H. 1983 Notes on long-crested water waves. *J. Fluid Mech.* **135**, 323–335.

ROBERTS, A. J. & SCHWARTZ, L. W. 1983 The calculation of nonlinear short-crested gravity waves. *Phys. Fluids* **26**, 2388–2392.

ZAKHAROV, V. E. 1968 Stability of periodic waves of finite amplitude on the surface of a deep fluid. *Z. Angew. Math. Phys.* **9**, 86–94.

ZHANG, J. & MELVILLE, W. K. 1987 Three-dimensional instabilities of nonlinear gravity-capillary waves. *J. Fluid Mech.* **174**, 187–208.